

Security and Privacy Enhanced Gait Authentication with Random Representation Learning and Digital Lockers

Lam Tran^a, Thuc Nguyen^b, Hyunil Kim^c, Deokjai Choi^{a,*}

^a*Artificial Intelligence Convergence Department, Chonnam National University, South Korea*

^b*Computer Science Department, Ho Chi Minh University of Sciences, Vietnam*

^c*Robotics Engineering Department, Daegu Gyeongbuk Institute of Science & Technology, South Korea*

Abstract

Gait data captured by inertial sensors have demonstrated promising results on user authentication. However, most existing approaches stored the enrolled gait pattern insecurely for matching with the validating pattern, thus, posed critical security and privacy issues.

In this study, we present a gait cryptosystem that generates from gait data the random key for user authentication, meanwhile, secures the gait pattern. *First*, we propose a revocable and random binary string extraction method using a deep neural network followed by feature-wise binarization. A novel loss function for network optimization is also designed, to tackle not only the intra-user stability but also the inter-user randomness. *Second*, we propose a new biometric key generation scheme, namely Irreversible Error Correct and Obfuscate (IECO), improved from the Error Correct and Obfuscate (ECO) scheme, to securely generate from the binary string the random and irreversible key. The model was evaluated with two benchmark datasets as OU-ISIR and whuGAIT. We showed that our model could generate the key of 139 bits from 5-second data sequence with zero False Acceptance Rate (FAR) and False Rejection Rate (FRR) smaller than 5.441%. In addition, the security and user privacy anal-

*Corresponding author

Email address: dchoi@jnu.ac.kr (Deokjai Choi)

yses showed that our model was secure against existing attacks on biometric template protection, and fulfilled irreversibility and unlinkability.

Keywords: gait authentication, biometric template protection, biometric cryptosystems, gait recognition, key binding scheme, biometric key generation.

1. Introduction

Along with the evolution of microelectromechanical technology, inertial sensors (*e.g.*, accelerometer, gyroscope) have been widely used and integrated into common mobile devices (*e.g.*, smartphone, smartwatch). This enables a practical, low-cost, and implicit mobile user authentication method, in which, the walking data captured by inertial sensors are exploited as the information sources to verify the user [1]. The first inertial sensor-based gait recognition model was proposed by Ailisto in [2]. After that, many studies have been conducted and confirmed the promising of this approach [1, 3, 4]. However, existing models require storing the enrolled gait patterns in plaintext for matching with the verified data, thus pose critical security and privacy issues.

Biometric cryptosystems (BCSs) refer to the techniques that either generate a secret key from biometric data, or use biometric data to seal a random secret key [5]. In this approach, user authentication is carried out indirectly by matching the key that represent the encrypted biometric data. Thus, the user privacy is also protected. Moreover, by using the key, BCS allows integrating biometric models to cryptographic schemes (*e.g.*, symmetric encryption). Several gait cryptosystems have been proposed (*e.g.*, [6, 7]) and demonstrated the potential of using BCS for gait, unfortunately, existed certain limitations. *First*, they relied on Fuzzy Commitment Scheme (FCS) [8] which has been specified as an unsecured solution when being deployed multiple times using the same biometric modality [9, 10, 11, 12]. *Second*, unlinkability and irreversibility, specified as the mandatory requirements to ensure the user privacy [13], however, were not addressed in [6, 7]. *Third*, the gait patterns were formed from the handcrafted features which had high intra-user variation and low inter-user discriminability,

thus, existing models were inefficient and low authentication performance.

It is worth noting that, constructing a BCS model is such a challenging task, as it needs to resolve five difficulties as follows [5, 13]. *Correctness*: The enrolled user should be able to reproduce the generated key with high probability. This is a challenging requirement, as the keys are required to match completely, however, biometric data always contain some variations. *Secure-ness*: Only the enrolled user is able to reproduce his generated key. In addition, the keys generated from different users must be random from each other. However, biometric data of different users usually show some common properties, and highly correlate to each other (*i.e.*, not totally random as the key’s expectation). *Revocability*: User should be able to change the key proactively, like changing a password. This contradicts to biometric data which are persistent for a long time period. *Irreversibility*: It is computationally impractical to learn the biometric data from the keys and/or the public data (*e.g.*, auxiliary data). *Unlinkability*: It is infeasible to identify with high certainty whether two given keys were constructed from the same or different users.

In this study, we propose a novel gait cryptosystem that securely and efficiently generates high-entropy keys from gait data, to be used for user authentication, and protects the user privacy. *First*, we observed that, raw gait data feature great intra-class variation but low inter-class discrimination which pose primary obstacles to achieve correctness and secureness. To address this, we propose a deep neural network that effectively extracts stable and discriminative features from raw gait data. The network is optimized using a new loss function which addresses not only the intra-class variation and inter-class discrimination of the extracted features, but also the randomness of the binary string derived from these features. *Second*, we present Irreversible Error Correct and Obfuscate (IECO), a BCS improved from Error Correct and Obfuscate (ECO) scheme [14], to securely generate a random and irreversible key from the gait binary string. The IECO scheme ensures the irreversibility which could not be achieved by ECO construction. Moreover, we adopt random projection [15] as an extra protection layer, to provide revocability and unlinkability.

In summary, our contributions in this study are:

- We proposed a method for extracting random binary string from gait segment using deep learning followed by feature-wise binarization. The network was optimized by a novel loss function that tackles not only the intra-user stability and inter-user separability, but also the inter-user randomness (see 4.2). Thus, the binary string extracted by our method is more random comparing to existing solutions (see 5.3.1).
- We introduced IECO, a new BCS that securely generates random and irreversible keys from biometric data (see 4.3). Theoretical and experimental analyses on secureness and correctness of IECO were also conducted, to serve as an instruction for parameter fine-tuning (see 4.4.3, 5.3.2).
- We conducted comprehensive experiments on the benchmark gait datasets (*i.e.*, OU-ISIR [16], whuGAIT [17]). The experimental results showed that our model can generate a key of 139 bits from 5-second gait segment with zero FAR, and the FRR of 4.167%, 5.441% for OU-ISIR, whuGAIT datasets, respectively (see 5.2). We provided detailed security analyses for our scheme under practical attacks. In addition, irreversibility and unlinkability evaluations were also conducted, and showed that our model could reliably protect the user privacy (see 5.4).

Note that, the objective of this study is different from the gait-based pairwise key generation researches which are well-summarized in [18]. In those studies, a nonce (*i.e.*, key) is generated from gait data, to establish a secure communication channel between multiple devices wearing by a same person. On the other hand, we generate a key, to be used for user authentication (before granting access to a service/resource). The objectives of two tasks are different, and each task has its own challenges and requirements to be addressed [18].

2. Related work

This section briefly reviews the related researches on gait authentication and
85 biometric cryptosystem.

2.1. Gait Authentication

Gait recognition research was initiated with computer vision techniques [19, 20]. This approach offered a solution for video surveillance or access control in a specific area (*e.g.*, building entrance) [3]. The evolution of sensing technology enabled a new gait recognition approach, which used the walking data
90 obtained by Inertial Measurement Units (IMUs) attached on user's body [2]. This approach is promising for continuous user authentication on mobile devices [3]. Many IMUs-based gait recognition studies have been conducted in the literature (*e.g.*, [1, 3, 7, 21, 22, 23, 24]). In the early stage, acceleration signals
95 were used as main data source (*e.g.*, [2, 25, 26]). The later researches additionally exploited the rotation rates obtained by gyroscope sensor to improve the performance (*e.g.*, [27, 22]). Moreover, some studies utilized multiple sensors placed in different positions of the user's body (*e.g.*, [28, 29]). Unfortunately, these studies did not provide any solution to protect the gait pattern, thus raised
100 critical privacy and security issues [5]. Our preliminary works demonstrated the potential of using BCS for gait authentication [6, 7], however, existed several limitations on performance as well as security and privacy.

2.2. Biometric Cryptosystem

Several generic Biometric Cryptosystem (BCS) frameworks have been proposed, to allow associating noisy data with a secret key. The first framework
105 proposed, to allow associating noisy data with a secret key. The first framework was proposed by Juels *et al.* [8], named Fuzzy Commitment Scheme (FCS). The main idea of FCS is to use biometric data to seal (*i.e.*, bind) a random binary key, then adopt error correcting code (ECC) [30] to handle the variation of biometric data. After that, Dodis *et al.* [31] introduced Fuzzy Extractor Scheme
110 (FES), which was a generalization of FCS. Another scheme proposed by Dodis was Fuzzy Vault Scheme (FVS) [32], that allowed sealing and revealing a secret

key using sets of unordered biometric features. Despite their effectiveness, these schemes exist certain vulnerabilities and suffer from several attacks when being deployed multiple times [9, 10, 11, 12]. In other words, these schemes could not
115 ensure unlinkability and irreversibility [13], thus could not remain secure when being deployed multiple times with the same biometric modality [9, 33].

The later BCS models mainly focused on enabling reusability (*a.k.a.*, revocability) (*e.g.*, [34, 35, 14]). Boyen introduced a first reusable BCS framework, however, it relied on an impractical assumption that required no sensitive information was revealed from the exclusive OR (XOR) of the enrolled templates [34].
120 Recently, Canetti *et al.* [14] introduced three fuzzy extractor schemes relying on Digital Lockers [36]. Among them, the first scheme, namely Sample Then Lock (STL) has been proved to be reusable under no assumption. However, STL requires extremely large storage space for the helper data [37, 38]. The
125 remaining two models, namely Error Correct and Obfuscate (ECO) and Condense then Fuzzy Extract (CFE), are not reusable. Several studies attempted to reduce the helper data size in the STL model [37, 38]. In [37], a threshold-based secret sharing scheme [39] was adopted to increase the error handling capability of the STL model, thus, significantly improved the storage efficiency, unfortunately, also increased the computational cost. The work in [38] used
130 ECC before adopting STL, to efficiently reduce the storage size. However, this approach stored the offset between the biometric template and codeword for key reproduction. This leads to several vulnerabilities as in FES and FCS.

Meanwhile, many BCS models on real biometric data have been proposed
135 (*e.g.*, fingerprint [40], face [41], face and iris [42], gait [6, 7]). Most initial studies focused on extracting from biometric data the deterministic and unique information, to be used as the key (*e.g.*, [6, 7, 40]). The later works started to address the revocability, unlinkability, and irreversibility (*e.g.*, [41, 42]).

3. Background

140 3.1. Digital Locker and Obfuscated Point Function

Digital Lockers (DL) are the symmetric encryption schemes that are computationally secure under multiple using times even with correlated and weak keys [36]. Let s be a secret key and v be a value. We mean $p = \text{dLock}(s, v)$ as a DL algorithm that locks v to p using the key s , and $\text{dUnlock}(s', p)$ as an unlock algorithm which returns v if $s' = s$, otherwise \perp with high probability. 145 With DL, obtaining any information of v given p is computationally difficult as guessing s . In addition, a wrong s' can be recognized with high probability. We used the DL construction proposed in [43]. The lock function is $\text{dLock}(s, v) = \{\text{nonce}, \text{H}(\text{nonce} \| s) \oplus (v \| 0^\gamma)\}$, where $\text{H}(\cdot)$ is a cryptographic hash 150 function, nonce is a nonce, and γ is the security parameter. Specifically, the algorithm can verify the correctness of s' with the certainty of $1 - 2^{-\gamma}$.

Obfuscated Point Function (OPF) is a special DL, in which, the plaintext is empty (*i.e.*, $v = \emptyset$). We use $p = \text{opLock}(s)$ as the OPF locking process. Then, the unlock function $\text{opUnlock}(s', p)$ will return 1 if $s' = s$, and 0 otherwise.

155 3.2. Error Correcting Code

Error Correcting Codes (ECC) are the algorithms for constructing sequences of numbers in special ways so that any errors occurring after that (up to a certain number) can be corrected. We use a family of ECC named BCH code [30], which allows correcting errors in any positions of the corrupted codeword. Let z and t 160 be two positive integers satisfying $z \geq 3$ and $t < 2^{z-1}$. There exists a BCH code, denoted as $C(n, k, t)$, consisted of 2^k codewords c of length n , where $n = 2^z - 1$, and k satisfies $n - k \leq zt$. Given any $m \in \{0, 1\}^k$, we mean $c \leftarrow \text{encode}_C(m)$ as encoding m to get $c \in C$. Let $c' \in \{0, 1\}^n$ be an error version of c such that $\text{d}_H(c', c) \leq t$, where $\text{d}_H(\cdot, \cdot)$ is the Hamming distance of the given strings. Then, 165 decoding c' can correct all the errors to get m (*i.e.*, $m \leftarrow \text{decode}_C(c')$).

3.3. Error Correct and Obfuscate Scheme

Algorithm 1 Key generation following ECO construction.

Input: the biometric template \mathbf{s} ;

Output: the generated key m ; the set of locked points \mathcal{P} ;

```

1:  $m \stackrel{\$}{\leftarrow} \{0, 1\}^k$ ;
2:  $c \leftarrow \text{encode}_C(m)$ ;
3: for  $i := 1$  to  $n$  do
4:   if  $c_i == 1$  then
5:      $p_i \leftarrow \text{opLock}(s_i)$ ;
6:   else
7:      $r_i \stackrel{\$}{\leftarrow} \mathcal{Z}$ ;
8:      $p_i \leftarrow \text{opLock}(r_i)$ ;
9:   end if
10:   $\mathcal{P} \leftarrow \mathcal{P} \cup p_i$ ;
11: end for
12: return  $\{\mathcal{P}, m\}$ ;

```

Algorithm 2 Key reproduction of the ECO construction.

Input: the biometric template \mathbf{s}' ; the set of locked points \mathcal{P} ;

Output: the reproduced key m' ;

```

1: for  $i := 1$  to  $n$  do
2:   if  $\text{opUnlock}(s'_i, p_i) == 1$  then
3:      $c'_i \leftarrow 1$ ;
4:   else
5:      $c'_i \leftarrow 0$ ;
6:   end if
7: end for
8:  $m' \leftarrow \text{decode}_C(c')$ ;
9: return  $m'$ ;

```

Error Correct and Obfuscate (ECO) is a fuzzy extractor scheme proposed by Canetti *et al.* [14], allows generating a random key from biometric template represented by a symbol string.

170 Let \mathcal{Z} be the symbol space (*e.g.*, $\mathcal{Z} = \{0, 1\}^\phi$, where ϕ is a small integer number). Let a biometric template be represented as $\mathbf{s} = [s_1 \ \dots \ s_i \ \dots \ s_n]$, where $s_i \in \mathcal{Z}$. The main idea of ECO is *obfuscation* that locks either a biometric symbol s_i or a random symbol $r_i \in \mathcal{Z}$ for each bit of the codeword (encoded from the key), according to the value of that bit. Without the key, it is unable
175 to tell whether a given locked point is from a random symbol r_i or a biometric symbol s_i . The key generation process that outputs a key $m \in \{0, 1\}^k$ and some

helper data from \mathbf{s} is summarized in algorithm 1. Then, given another biometric template \mathbf{s}' , the key m' could be reproduced as in algorithm 2.

ECO also utilizes ECC to handle the variation of biometric data, similar to FES. However, in ECO, the distance between biometric template and the code word is not stored as in FES. Thus, the attacks on FES that exploit the helper data and ECC [9], could not work on ECO model. Despite the improvement, ECO does not offer reusability [14] (see 4.4.4).

4. Gait Cryptosystem Framework

Overview. Figure 1 sketches the overall model architecture, which operates in two phases, each phase is processed through four blocks.

Key generation (i.e., enrollment): First, the Preprocessing Block preprocesses and splits the raw data sequence into suitable segments. Then, the Deep Feature Extraction (DFE) block extracts from the gait segment a representative feature vector \mathbf{f} of length N . Subsequently, the Revocable String Forming (RSF) block transforms \mathbf{f} using random projection, then binaries the transformed template to a revocable bit string ω with the sign function. By random projection, multiple instances of ω could be produced, to enable key revocability. Finally, the Irreversible Error Correct and Obfuscate (IECO) block generates a key κ from ω . Note that, in this phase, some helper data are extracted and publicly stored for key reproduction. We show that it is impractical to learn neither the gait data nor the key from these data.

Key reproduction (i.e., validation): The same processing blocks are performed on new gait data to obtain a key κ' , under the assistance of the helper data. We now describe each processing block in detail.

4.1. Data Preprocessing Block

We use acceleration and gyroscope signals as the data source for key generation. The data preprocessing and segmentation methods are referred from [44], which are summarized as follows.

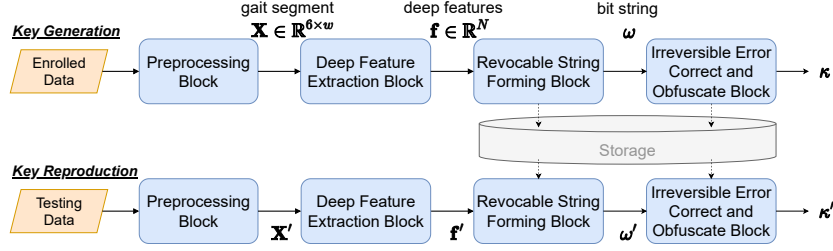


Figure 1: The processing blocks of our sensors-based gait cryptosystem.

205 Let $\mathbf{A} = [\mathbf{a}_{t_1} \quad \mathbf{a}_{t_2} \quad \dots \quad \mathbf{a}_{t_i} \quad \dots]$ be a sequence of acceleration signals, where $\mathbf{a}_{t_i} = [a_{t_i}^X \quad a_{t_i}^Y \quad a_{t_i}^Z]^\top$ represents the acceleration forces acting along the X , Y , and Z axes at the time t_i . Similarly, we use $\mathbf{G} = [\mathbf{g}_{t'_1} \quad \mathbf{g}_{t'_2} \quad \dots \quad \mathbf{g}_{t'_i} \quad \dots]$ to represent a sequence of gyroscope signals, where $\mathbf{g}_{t'_i} = [g_{t'_i}^X \quad g_{t'_i}^Y \quad g_{t'_i}^Z]^\top$ represents the rotation rates around the X , Y , and Z axes at the time t'_i . The raw gyroscope signals are interpolated with respect to the acting time of acceleration signals [45], to overcome the asynchrony between the gyroscope and accelerometer. Then, we combine the acceleration and gyroscope sequences to a six-channel data stream $[\mathbf{x}_{t_1} \quad \mathbf{x}_{t_2} \quad \dots \quad \mathbf{x}_{t_i} \quad \dots]$, where $\mathbf{x}_{t_i} = [a_{t_i}^X \quad a_{t_i}^Y \quad a_{t_i}^Z \quad g_{t_i}^X \quad g_{t_i}^Y \quad g_{t_i}^Z]^\top$. The data stream is broken into fixed-length segments of w signals, where w is the window size, chosen so that each segment contains at least one gait cycle.

210

215

4.2. Deep Feature Extraction Block

Let \mathbf{X} denote a gait data segment output by the Preprocessing Block. In the DFE block, a deep network is used to extract a representative template \mathbf{f} from \mathbf{X} . This section first presents the network architecture, then describes the loss function for network optimization.

220

4.2.1. Network Architecture

The overall network architecture comprises of two branches as Convolutional Neural Network (CNN) and Long Short-term Memory (LSTM) network, extracting the features independently (see Figure 2).

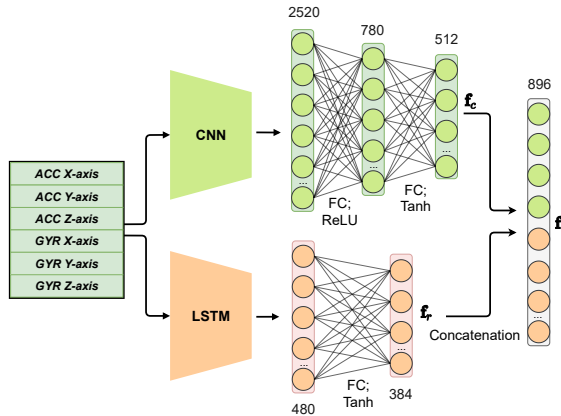


Figure 2: The deep network for extracting deep features from gait segment, where CNN is from [46] and LSTM is from [44].

- 225
230
235
 • *CNN*: This branch extracts a spatial feature template \mathbf{f}_c from the gait segment \mathbf{X} . We leverage the CNN architecture proposed in [46] and make appropriate modifications for extracting representative template. Specifically, from the original network, we discard the last softmax layer, then add two fully-connected (FC) layers. The first FC layer scales the feature dimension from 2520 to 780, and uses rectified linear unit (ReLU) as the activation function. The second FC layer computes the representative template \mathbf{f}_c of size 512 from the output of the first FC layer. In this layer, \tanh is used as the activation function to scale the feature value to the range $(-1, 1)$.
- *LSTM*: We utilize the LSTM network proposed in [44] for extracting from \mathbf{X} the temporal features \mathbf{f}_r . We also discard the last softmax layer of the original network, then, add a new FC layer, to map the extracted features to a template \mathbf{f}_r of size 384. \tanh also is used as the activation function.

The representative template \mathbf{f} is formed by concatenating \mathbf{f}_r and \mathbf{f}_c , $\mathbf{f} = \mathbf{f}_c \parallel \mathbf{f}_r$.

4.2.2. Random Representation Learning

Each branch of the network is trained separately, using the same optimization method. Here, to simplify the notation, we use \mathbf{f} as the output of CNN or

LSTM network (*i.e.*, $\mathbf{f} = \mathbf{f}_c$, or $\mathbf{f} = \mathbf{f}_r$) when explaining the optimization method.

Several optimization functions have been proposed to extract representation string for image retrieval (*e.g.*, [47, 48]). However, these studies addressed
 245 the task of semantic-preserving representation learning, in which, the Hamming distance of the extracted strings should reflect the similarity of the information sources. Such methods are inappropriate to be used in a BCS model. A secure BCS model expects that, (*I*) the binary strings extracted from the same user
 250 should be close to each other, and (*II*) those from different users should randomly differ 50% (*i.e.*, differ from each other 50%, and the different positions are random and unpredictable). The requirement (*II*) is critically important, and strongly affects the model’s security.

We introduce a new optimization function for learning the representative
 255 templates \mathbf{f} so that the binary string ω obtained from \mathbf{f} satisfies two requirements above. First, we consider the triplet loss [49] which optimizes the feature templates to be close when extracted from same user, and far for different users. Let \mathbf{f}_u and \mathbf{f}'_u be two feature templates extracted from a user u , and \mathbf{f}_v be the template of another user $v \neq u$. Then, the triplet loss is computed as:

$$L_T = \max(\mathbf{d}_E(\mathbf{f}_u, \mathbf{f}'_u) - \mathbf{d}_E(\mathbf{f}_u, \mathbf{f}_v) + \delta, 0), \quad (1)$$

260 where $\mathbf{d}_E(\cdot, \cdot)$ means the Euclidean distance, and δ is the desired margin. By minimizing L_T , $\mathbf{d}_E(\mathbf{f}_u, \mathbf{f}'_u)$ is pushed to zero, and $\mathbf{d}_E(\mathbf{f}_u, \mathbf{f}_v)$ tends to be larger than $\mathbf{d}_E(\mathbf{f}_u, \mathbf{f}'_u) + \delta$. The use of triplet loss solves the requirement (*I*) and pushes the templates of different users as far as the margin δ , however, could not ensure the requirement (*II*). To address this, we propose additional criterion as follows.
 265 As \tanh is used as the activation function in the last layer (see 4.2.1), the value of each feature is scaled to the range $(-1, 1)$. Let $f_{u,i}$ and $f_{v,i}$ be the feature i of \mathbf{f}_u and \mathbf{f}_v , respectively. As sign is used as the binarization function (see 4.3.2), two users u and v will have a same bit i if $f_{u,i}f_{v,i} > 0$, and different bit if $f_{u,i}f_{v,i} < 0$. Thus, to achieve (*II*), the number of positions having $f_{u,i}f_{v,i} > 0$
 270 should be approximate to the number of positions having $f_{u,i}f_{v,i} < 0$. This can

be performed by minimizing

$$L_R = \left| \sum_{i=1}^N f_{u,i} f_{v,i} \right| = |\langle \mathbf{f}_u, \mathbf{f}_v \rangle|, \quad (2)$$

where $\langle \cdot, \cdot \rangle$ is the inner product. Combining (1) and (2), we have

$$L = \max(\alpha d_E(\mathbf{f}_u, \mathbf{f}'_u) - d_E(\mathbf{f}_u, \mathbf{f}_v) + \beta |\langle \mathbf{f}_u, \mathbf{f}_v \rangle| + \delta, 0), \quad (3)$$

where α and β are the regularization parameters. By minimizing L , the feature templates of the same user will get closer (due to the constraint of $d_E(\mathbf{f}_u, \mathbf{f}'_u)$), thus the intra-class variation of the binary string ω is also reduced. Meanwhile, the feature templates of different users will be more different in a way that the number of positions having $f_{u,i} f_{v,i} > 0$ is approximate to the number of cases having $f_{u,i} f_{v,i} < 0$ (due to the constraint $-d_E(\mathbf{f}_u, \mathbf{f}_v) + |\langle \mathbf{f}_u, \mathbf{f}_v \rangle|$).

4.3. Revocable String Forming Block

The Revocable String Forming (RSF) block transforms \mathbf{f} to a revocable binary string $\omega \in \{0, 1\}^{\phi n}$, where ϕ is the symbol size, and n is the codeword length (see 4.4). This task is performed in two steps as follows.

4.3.1. Random Projection

First, instead of using \mathbf{f} to generate the key, we adopt Random Projection (RP) to provide revocability. RP is a dimensional reduction technique inspired from the Johnson-Lindenstrauss Lemma [15], which allows projecting vector templates into a random sub-space while approximately preserving their pairwise similarity. Specifically, given a feature template $\mathbf{f} \in \mathbb{R}^N$, we project it to a K -dimensional vector $\hat{\mathbf{f}}$ as $\hat{\mathbf{f}} = \mathbf{f} \times \mathbf{R}$, where $K = N - 1$, and \mathbf{R} is an $N \times K$ matrix whose entries are independent and identically distributed according to a Gaussian distribution of zero mean and $\frac{1}{N}$ variance. After this step, $\hat{\mathbf{f}}$ is used to generate the key while \mathbf{f} is discarded.

4.3.2. Binarization and Reliable Bits Selection

To increase the stability, M projected templates (derived from M segments
 295 projected with the same RP matrix) are used to construct one binary string.
 For each feature i ($1 \leq i \leq K$), we compute the mean $\bar{f}_i = \frac{1}{M} \sum_{j=1}^M \hat{f}_i^j$, where \hat{f}_i^j is
 the feature i of the projected template $\hat{\mathbf{f}}^j$ ($1 \leq j \leq M$). Then, ω_i is determined:

$$\omega_i = \text{sign}(\bar{f}_i) = \begin{cases} 1 & \text{if } \bar{f}_i \geq 0, \\ 0 & \text{otherwise.} \end{cases} \quad (4)$$

Subsequently, we statistically select ϕn reliable bits which have low intra-class
 error. The reliability of a feature is computed by $r_i = -\frac{1}{M-1} \sum_{j=1}^M (\hat{f}_i^j - \bar{f}_i)^2$.
 300 Then, ω is formed from ϕn bits having highest reliability.

4.4. Irreversible Error Correct and Obfuscate Block

We present here the IECO scheme, which generates from ω an irreversible
 key κ . The overall idea of IECO is to use a nonce m to lock the key κ by a DL,
 then use the reliable string ω to seal m following the ECO construction.

305 4.4.1. Key Generation

Let ϕ be the symbol size, *i.e.*, $\mathcal{Z} = \{0, 1\}^\phi$. Given ω , a symbol string $\mathbf{s} \in \mathcal{Z}^n$
 is constructed to be used as the input of the IECO scheme, where each symbol
 s_i is formed from ϕ consecutive bits of ω , $s_i = \omega_{(i-1)\phi+1} \parallel \dots \parallel \omega_{i\phi}$. Then, a key
 κ is generated from \mathbf{s} as follows:

- 310 (i) First, $\kappa \in \{0, 1\}^k$ is generated randomly.
- (ii) Next, a nonce $m \in \{0, 1\}^k$ is encoded to a codeword c , $c \leftarrow \text{encode}_C(m)$.
 Meanwhile, m is used to lock the key κ to L_κ using a DL, $L_\kappa \leftarrow \text{dLock}(m, \kappa)$.
- (iii) For each bit c_i ($1 \leq i \leq n$), a locked point p_i is created

$$p_i = \begin{cases} \text{opLock}(s_i) & \text{if } c_i = 1, \\ \text{opLock}(r_i) & \text{otherwise,} \end{cases} \quad (5)$$

Algorithm 3 Key generation using IECO scheme.

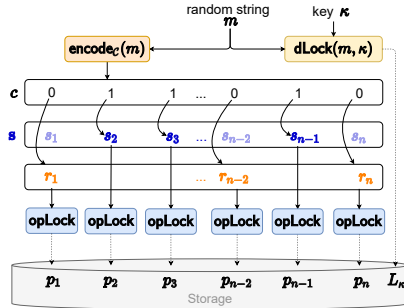
Input: the symbol string s ;

Output: the generated key κ ; the locked points \mathcal{P} .

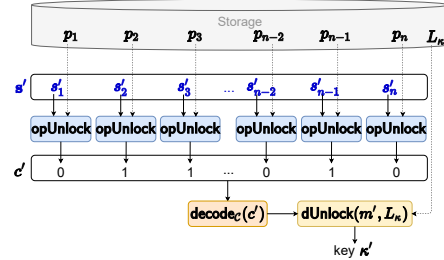
```

1:  $\kappa \xleftarrow{\$} \{0, 1\}^k$ ;
2:  $m \xleftarrow{\$} \{0, 1\}^k$ ;
3:  $L_\kappa \leftarrow \text{dLock}(m, \kappa)$ ;
4:  $c \leftarrow \text{encode}_C(m)$ ;
5: for  $i := 1$  to  $n$  do
6:   if  $c_i == 1$  then
7:      $p_i \leftarrow \text{opLock}(s_i)$ ;
8:   else
9:      $r_i \xleftarrow{\$} \{z \in \mathcal{Z} | z \neq s_i\}$ ;
10:     $p_i \leftarrow \text{opLock}(r_i)$ ;
11:   end if
12:    $\mathcal{P} \leftarrow \mathcal{P} \cup p_i$ ;
13: end for
14: return  $\{\mathcal{P}, L_\kappa, \kappa\}$ ;

```



(a) Key generation.



(b) Key reproduction.

Figure 3: An illustration of key generation and reproduction following the IECO construction.

where r_i is generated randomly from \mathcal{Z} so that $r_i \neq s_i$. We store L_κ and p_i for key reproduction, while s , m , κ and r_i are discarded.

315

We provide the pseudo-code for the key generation process in Algorithm 3, and depict an example in Figure 3a.

4.4.2. Key Reproduction

Given a validating binary string ω' , a symbol string s' is constructed. Then, s' is used to reproduce the generated key as follows:

320

Algorithm 4 Key reproduction with the IECO scheme.

Input: the biometric template s' ; the set of locked points \mathcal{P}, L_κ .

Output: the reproduced key κ' .

```

1: for  $i := 1$  to  $n$  do
2:   if  $\text{opUnlock}(s'_i, p_i) == 1$  then
3:      $c'_i \leftarrow 1$ ;
4:   else
5:      $c'_i \leftarrow 0$ ;
6:   end if
7: end for
8:  $m' \leftarrow \text{decode}_C(c')$ ;
9:  $\kappa' \leftarrow \text{dUnlock}(m', L_\kappa)$ ;
10: return  $\kappa'$ ;

```

(i) First, each bit of the codeword c' is determined

$$c'_i = \begin{cases} 1 & \text{if } \text{opUnlock}(s'_i, p_i) = 1, \\ 0 & \text{otherwise.} \end{cases} \quad (6)$$

(ii) Then, a nonce m' is obtained from c' by $m' \leftarrow \text{decode}_C(c')$.

(iii) Finally, κ' is retrieved as $\kappa' \leftarrow \text{dUnlock}(m', L_\kappa)$. In this step, κ' is identical to κ if $m' = m$, otherwise $\kappa' = \emptyset$ with the certainty of $1 - 2^{-\gamma}$.

325 Algorithm 4 summarizes the pseudo-code for key reproduction, and Figure 3b sketches an example of it.

4.4.3. Correctness and Secureness Analysis

In this section, we analyze the impact of IECO's parameters to the correctness and secureness, to provide instructions for parameter fine-tuning.

330 **Correctness:** Correctness is decided by the ability of tolerating the intra-user biometric variation to generate a deterministic key. Thus, we analyze the variation tolerability of IECO with respect to its parameters, then, the correctness could be inferred.

Let ω and ω' be the strings extracted from the same user. Let ζ be the probability of a bit i to be error (*i.e.*, $P_{(\omega'_i \neq \omega_i)} = \zeta$). For simplicity, we assume 335 the errors can independently occur in any position with the same probability.

From the IECCO's construction, the key κ is successfully reproduced if $m' = m$ (assuming that the error of DL is negligible, *i.e.*, $2^{-\gamma} \approx 0$). This can be satisfied if $d_H(c', c) \leq t$. Thus, we can firstly see that, the variation tolerability is decided
 340 by the adopted ECC. On the other hand, c_i and c'_i can be different in two cases:

(i) $c_i = 1, c'_i = 0$: This occurs when $s_i \neq s'_i$ and $c_i = 1$ (*i.e.*, the position i that s_i is used to create p_i instead of using a random r_i). As each symbol s_i is formed from ϕ bits of ω , the probability of this case is

$$P_{(c'_i \neq c_i | c_i = 1)} = P_{(s'_i \neq s_i | c_i = 1)} = \frac{1}{2} \phi \zeta, \quad (7)$$

(assuming that the numbers of bit 1s and 0s in c are equal).

345 (ii) $c_i = 0, c'_i = 1$: For the position i having $c_i = 0$, an incorrect c'_i is returned if $s'_i = r_i$, where r_i is the random symbol generated in the key generation phase. The probability for this case is

$$P_{(c'_i \neq c_i | c_i = 0)} = P_{(s'_i = r_i | c_i = 0)} = \frac{1}{2} \frac{\phi \zeta}{(2^\phi - 1)}. \quad (8)$$

From (7) and (8), the probability of s_i to be different from s'_i is

$$P_{(c'_i \neq c_i)} = \frac{1}{2} \left(\phi \zeta + \frac{\phi \zeta}{(2^\phi - 1)} \right) = \frac{1}{2} \zeta \left(\phi + \frac{\phi}{2^\phi - 1} \right). \quad (9)$$

We could see that, with ζ as a constant, then $P_{(c'_i \neq c_i)}$ is represented as an in-
 350 creasing function with respect to $\phi \in \mathbb{N}^*$. So, under the same variation condition of biometric data (specified by ζ), increasing ϕ will increase the probability of error between c and c' , thus, reduce the model's correctness.

Secureness: We measure the impacts of IECCO's parameters on secureness. Let ω^u and ω^v be the strings extracted from users u and v , and κ be a key
 355 generated from ω^u . We analyze the probability of successfully reproducing κ using ω^v , with respect to the IECCO's parameters. We assume that $P_{(\omega_i^u = \omega_i^v)} = \eta$, $\forall i = 1.. \phi n$, where ω_i^u and ω_i^v are the bits i of ω^u and ω^v , respectively.

We could see that, user v can successfully obtain κ if $d_H(c^u, c^v) \leq t$, where

c^u is the codeword generated in the enrollment phase of user u , and c^v is the
 360 codeword reproduced by ω^v . Thus, the secureness is firstly decided by the
 error correcting capability t of the ECC, in which, increasing t will reduce the
 secureness. Next, we consider the impact of ϕ . There are two cases for $c_i^u = c_i^v$:

(i) $c_i^u = 1, c_i^v = 1$: This happens when $s_i^v = s_i^u$ and $c_i^u = 1$. As each symbol is
 formed from ϕ bits of ω , the probability of this case is

$$P_{(c_i^v=c_i^u|c_i^u=1)} = P_{(s_i^v=s_i^u|c_i^u=1)} = \frac{1}{2}\eta^\phi. \quad (10)$$

365 (ii) $c_i^u = 0, c_i^v = 0$: This happens when $c_i^v = 0$ and $s_i^v = r_i$, where r_i is the
 random symbol generated in the key generation phase. The probability of
 this case is

$$P_{(c_i^v=c_i^u|c_i^u=0)} = P_{(s_i^v \neq r_i|c_i^u=0)} = \frac{1}{2}(\eta^\phi + (1 - \eta^\phi)\frac{2^\phi - 2}{2^\phi - 1}). \quad (11)$$

In summary, the probability for c_i^u to be equal to c_i^v is

$$P_{(c_i^v=c_i^u)} = \eta^\phi + \frac{1}{2}(1 - \eta^\phi)\frac{2^\phi - 2}{2^\phi - 1}. \quad (12)$$

We can see that $\lim_{\phi \rightarrow \infty} P_{(c_i^v=c_i^u)} = 0.5$. That means, when increasing the symbol
 370 size ϕ , the probability of a bit c_i^v to be equal to c_i^u will approach 0.5, thus, it is
 more difficult a user to reproduce the key generated by another user.

In conclusion, the model's correctness and secureness are controlled by:

- *Error correcting capability t* : Increasing t will increase the correctness,
 however, decrease the model's secureness.
- 375 • *Symbol size ϕ* : Increasing ϕ will lead to a more secure model, however,
 decrease the model's correctness.

4.4.4. Security and Privacy Improvement

Here, we describe the security improvement over the original scheme.

Weakness of ECO: The ECO scheme could not ensure irreversibility, thus,
 380 it is a non-reusable scheme. Specifically, with the construction described in 3.3,
 we assume that the key m is compromised. Then, the attacker could determine
 the used codeword c as $c = \text{encode}_C(m)$. By observing c , he can identify which
 locked points p_i are derived from the biometric symbols. Subsequently, given a
 locked point p_i , the sealed symbol s_i could be identified with the computational
 385 cost as 2^ϕ . As ϕ is usually small, s_i could be effectively obtained by exhaustively
 searching all possible values in \mathcal{Z} . When sufficient components of \mathbf{s} are known,
 the attacker can compromise all other keys generated from the same user.

Our improvement: In IECO, instead of using m as the generated key,
 we use m to lock κ with a DL. κ is output as the generated key while m is
 390 discarded. In case of κ is compromised, L_κ and κ provide no information to
 compute m [36]. Guessing m from κ and L_κ is equivalent to brute force all
 possible values of m . Thus, when κ is compromised, the adversary gains no
 advantage in reconstructing the biometric data.

5. Experimental Evaluation

395 In this section, we present the experimental evaluations for the proposed
 model. First, we explain the datasets and experiment procedure, then, report
 the performance under optimal parameters. In addition, we analyze the adopted
 techniques in details, and present the evaluations on security and user privacy.
 Finally, a relative comparison to existing researches is provided.

400 5.1. Experiment Procedure

Our model was evaluated with OU-ISIR [16] and whuGAIT datasets [17].

5.1.1. OU-ISIR Dataset

OU-ISIR is known as the largest population public gait dataset, formed from
 the IMU-based gait data of 744 users. We divided this dataset into two non-
 405 overlapping sets for training and testing. The training set consisted of 520 users,
 and the testing set contained data of other 224 users.

Data sequences in the training set were split into segments of $w = 100$ signals. Two segments of each user formed a validating set \mathcal{V} , and all remaining segments formed a learning set \mathcal{L} . Note that, two consecutive segments in \mathcal{L} overlapped
410 each other 97%. \mathcal{L} is used to train the network from scratch, with the mini-
batch size of 128. The CNN branch was updated using Adam algorithm with the
learning rate as 15×10^{-6} . For the LSTM branch, Stochastic Gradient Descent
algorithm with the learning rate of 0.15 and momentum of 0.9 was used. When
415 completing an epoch, the validation loss over the set \mathcal{V} was computed. If
this loss did not decrease during 15 epochs, we terminated the training process.
Then, the network was used as a feature extraction tool to extract representation
template from the gait segment.

Data of 224 users in the testing set were used to build and evaluate 224
key generation models (one model for each user). Specifically, for each user u ,
420 his/her data were divided into two non-overlapping and equal parts. The gait
segments from the first part were used as the enrolled data to generate a key
 κ_u . Then, the remaining data of u , along with data of 223 other users, were
used to reproduce κ_u . To increase the stability of the reproduced key, we used 5
segments for each attempt. Specifically, given 5 gait segments, 5 representation
425 templates \mathbf{f}^i were extracted. Then, their mean template was determined and
used to reproduce the key. The performance was evaluated with FRR and FAR.
Let N_u be the number of times a user tried to reproduce his generated key, and
 F_u be the failed times. The FRR was determined as $\text{FRR} = \frac{F_u \times 100}{N_u}$. Let N_o be
the number of times that the data of other users were used to reproduce the
430 key, and F_o be the success times. The FAR was estimated as $\text{FAR} = \frac{F_o \times 100}{N_o}$.

5.1.2. WhuGAIT Dataset

WhuGAIT dataset consists of IMUs-based gait data of 118 users, acquired in
realistic conditions. We also divided this dataset into two non-overlapping sets
for training and testing. The training set consisted of 98 users, and the testing
435 set contained data of the remaining 20 users. Then, the experiment procedure
with this dataset was conducted similarly to the OU-ISIR dataset.

5.1.3. Parameter Fine-tuning

In (3), α and β need to be fine-tuned for optimal performance. Exhaustively trying all of their combinations is a computationally expensive task. Thus, we used an adaptive search that manually examined the output of a combination and adjusted the parameters accordingly. We started by training the model with $\alpha = \beta = 1$. The reliable strings ω were extracted and the histogram of normalized Hamming distance was estimated (as in Figure 5c). If the Hamming distance of intra-class was high, we increased the value of α by 0.1, while keeping β unchanged. By changing α , we could find a good trade-off between intra-class stability and inter-class separability. Then, we adjusted β (0.1 in each iteration) to balance the randomness and intra-class stability. By increasing β , the histogram of inter-class normalized Hamming distance would centralize to 0.5 harder, however, the intra-class Hamming distance would increase.

By the above process, we found that, the model achieved the best balance with $\alpha = 1.2$, $\beta = 0.9$ for OU-ISIR, and $\alpha = 1.1$, $\beta = 1.8$ for whuGAIT.

5.2. Overall Performance

Our scheme achieved the best performance when using IECO with BCH code of length 255 and symbol size $\phi = 2$. The detailed performances at different key sizes are summarized in Table 1 (on the assumption of ideal DL and OPF, *i.e.*, $2^{-\gamma} \approx 0$). We could see that, under the same settings of codeword length and symbol size, the key size k controls the trade-off between the FAR (*i.e.*, secureness) and FRR (*i.e.*, correctness). Increasing k will decrease the error correcting capability t of the code C , thus the FAR is reduced and FRR is increased. This confirms the analysis in 4.4.3.

Figures 4 show the normalized Hamming distance between the enrolled codeword c and the reproduced codewords c' . We could see that, when c' is reproduced by the enrolled user (intra-class), it showed low variation from c . On the other hand, when using the other users' data (inter-class), the distance between c' and c follows a Gaussian of mean approximated to 0.5.

Table 1: Performances at different key sizes when using BCH code of length 255 and symbol size $\phi = 2$.

<i>Key size</i> (bits)	<i>Error Tolerability</i>	<i>OU-ISIR</i>		<i>whuGAIT</i>	
		<i>FAR</i> (%)	<i>FRR</i> (%)	<i>FAR</i> (%)	<i>FRR</i> (%)
115	21	0.001	2.083	0.022	2.177
123	19	0	4.167	0.005	2.66
131	18	0	4.167	0	3.265
139	15	0	4.167	0	5.441
147	14	0	6.25	0	6.771

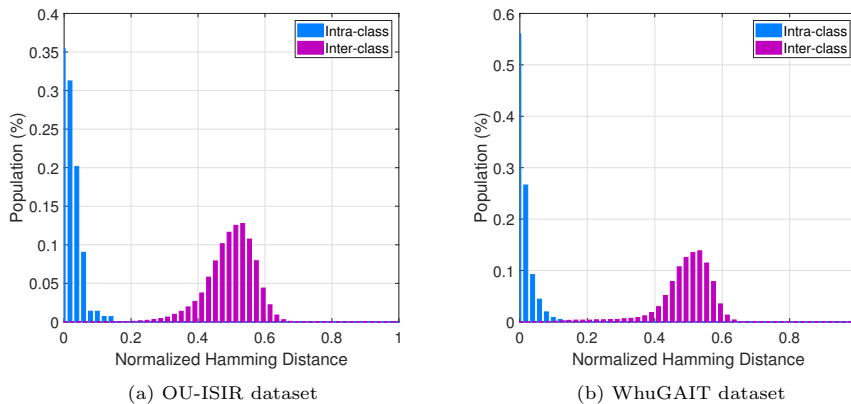


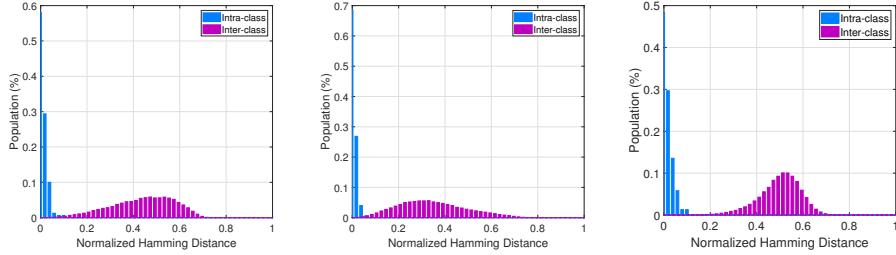
Figure 4: The normalized Hamming distance between the enrolled codeword c and the reproduced codewords c' .

5.3. Discussion

In this section, we provide detailed analyses for the adopted methods, to confirm their impacts on the overall performance and security.

5.3.1. Optimization Function

470 First, we compare our loss function with existing solutions (*i.e.*, [49, 42]).
 Figures 5 show the normalized Hamming distance of the reliable string ω extracted with different loss functions, measured on OU-ISIR dataset. With triplet loss [49], the strings extracted from a same user are highly stable, *i.e.*, the normalized intra-class Hamming distance distribution approximately follows a
 475 half-Gaussian of mean $\mu = 0$ and standard deviation $\sigma = 0.0156$ (Figure 5a).
 However, this loss function does not address the inter-class randomness (*i.e.*,



(a) The original triplet loss [49]. (b) The loss proposed in [42] (c) Our proposed loss function.

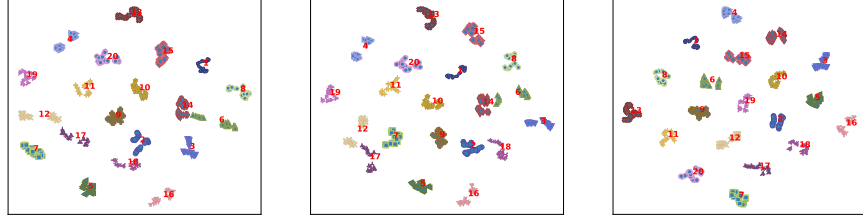
Figure 5: The normalized Hamming distance of the reliable binary strings ω when using our loss function in comparing to existing solutions.

inter-class Hamming distance follows a Gaussian of $\mu = 0.4365$ and $\sigma = 0.1703$). Poor inter-class randomness would cause the model to be vulnerable from several attacks (*e.g.*, statistical attack, nearest impostor attack) [50].

480 The study [42] proposed two constraints to improve the randomness and stability of the extracted binary string. The first one directs each feature to get closer to 1 or -1 , thus, increases its stability, $L_2 = \frac{1}{N} \sum_{i=1}^{|\mathcal{B}|} \|\mathbf{f}^i\|$ where $|\mathcal{B}|$ is the mini-batch size, and N is the length of the feature template. The second constraint aims to balance the numbers of bit 1 and 0 in the extracted string, 485 $L_3 = \frac{1}{N} \sum_{i=1}^{|\mathcal{B}|} \sum_{j=1}^N f_j^i$, where f_j^i is the feature j of template i . Figure 5b plots the normalized Hamming distance of ω when combining these constraints with triplet loss. Comparing to using only triplet loss, incorporating these constraints improves the intra-class stability (*i.e.*, σ is reduced to 0.0108). However, the inter-class separability and randomness are not improved.

490 With our loss function, although the stability of intra-class is minorly reduced (*i.e.*, the half-Gaussian for intra-class has $\mu \approx 0$ and $\sigma = 0.0251$), the inter-class randomness is remarkably increased (*i.e.*, $\mu = 0.496$ and $\sigma = 0.0871$).

Figures 6 plot the visualization of the representation vectors \mathbf{f} using t-Distributed Stochastic Neighbor Embedding (t-SNE) [51]. For the loss func- 495 tions [49, 42], although the representation vectors are grouped into separated clusters, some clusters still close to each other (*e.g.*, 2 and 18; 14 and 6; 12 and 17). With our loss function, the clusters are clearly separated from each other



(a) The original triplet loss [49]. (b) The loss proposed in [42] (c) Our proposed loss function.

Figure 6: T-SNE visualization of the extracted feature f of 20 testing users in OU-ISIR dataset.

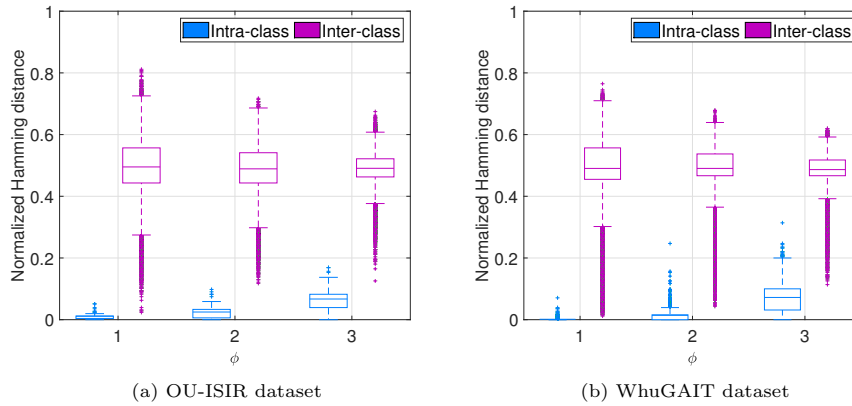


Figure 7: The normalized Hamming distance distribution measured on c under different settings of symbol size ϕ .

by a certain margin, and no cluster is too close to another.

5.3.2. Symbol size

500 We experimentally analyzed the impact of symbol size ϕ on the overall performance and security. Figures 7 display the Hamming distance between the enrolled codeword c and the reproduced codeword c' when using different symbol sizes. We observed that, when ϕ is increased, the intra-class Hamming distance is also increased, which means the error toleration capability is reduced. Meanwhile, increasing ϕ makes the inter-class Hamming distance to be
505 harder centralized around the mean 0.5, thus, increases the security. These observations confirm the theoretical analysis of ϕ in 4.4.3.

5.4. Privacy and Security Analyses

As specified in ISO/IEC standard [13], irreversibility and unlinkability are
510 mandatory for a biometric template protection solution. In this section, the
evaluations on irreversibility and unlinkability are provided. In addition, we
analyze the model security against practical attacks on BCS solutions.

5.4.1. Irreversibility

Irreversibility refers to the computational hardness of inferring biometric
515 data from the extracted helper data or/and the generated key.

First, we consider a scenario in which the extracted key κ has not been
compromised, and the attacker tries to infer the biometric features from the
extracted helper data. All the helper data include the deep network’s weights
and biases, the RP matrix \mathbf{R} , the reliable feature index, and the locked points
520 $\{\mathcal{P}, L_\kappa\}$. The network is not trained by the enrolled user’s data, and the repre-
sentative template is discarded after enrollment. Thus, it is impractical to infer
the enrolled user’s data from the network [52]. The RP matrix is randomly
generated, and is independent from the gait data (see 4.3), thus, it provides no
information to infer the gait data. Although the reliable feature index shows the
525 reliability order of extracted features, it is useless for guessing the actual value
of gait features. From each locked point $p_i \in \mathcal{P}$, the attacker can infer the in-
side plaintext with the computational complexity as 2^ϕ . As ϕ is a small number
(*i.e.*, $\phi = 2$ in our model), the value contained inside p_i can be obtained easily.
However, without c_i (which is unknown from the attacker), the attacker can not
530 determine whether p_i is the locked point of a biometric symbol s_i or a random
string r_i . There are $n = 255$ locked points, where n is the codeword length.
Thus, the complexity of guessing the biometric template given all locked points
is 2^{255} . L_κ is the locked point of κ using the key as m , (*i.e.*, $L_\kappa \leftarrow \text{dLock}(m, \kappa)$).
Given only L_κ , it is computationally impractical to obtain m [36].

535 Next, we consider a scenario in which the key κ has been compromised (*e.g.*,
user may mistakenly submit κ to a fake application). Given κ and L_κ , the only
way for the attacker to obtain m is guessing all possible values of m [36]. The

complexity of this task is $2^k = 2^{139}$, where k is the message length of the adopted BCH code, which is also the model’s security level. Thus, in our model, even
 540 the generated key κ has been compromised, the attacker still can not gain any additional advantage on reconstructing the original gait template.

5.4.2. Unlinkability

We adopted the framework proposed in [53] to evaluate the unlinkability. In this method, the *mated* and *non-mated* scores will be evaluated, to mea-
 545 sure the similarity of the extracted strings when changing only the parameters (*i.e.*, RP matrix), and when changing both the parameters and the biometric source. Then, two metrics are computed to evaluate the unlinkability. The first one is *local score-wise*, $D_{\leftrightarrow}(s) \in [0, 1]$, which reflects the likelihood ratio of mated and non-mated score distribution in a specific score. In a specific score,
 550 $D_{\leftrightarrow}(s) = 1$ means the system is fully linkable, while $D_{\leftrightarrow}(s) = 0$ implies the fully unlinkability. The second one is *global measure*, $D_{\leftrightarrow}^{sys} \in [0, 1]$, gives an overall quantification of the unlinkability. For a fully unlinkable model, $D_{\leftrightarrow}^{sys}$ should be close to zero.

With each user in the testing sets, we randomly generated 100 projection
 555 matrices, and used them to generate 100 reliable strings. From the generated strings, we calculated the mated and non-mated scores, as well as $D_{\leftrightarrow}(s)$ and $D_{\leftrightarrow}^{sys}$. Figures 8a display the unlinkability scores measured on OU-ISIR and whuGAIT datasets. By the small global measure scores (*i.e.*, 0.0028 and 0.0053 for OU-ISIR and whuGAIT, respectively), the unlinkability of our model is
 560 confirmed.

5.4.3. Security Analysis

We evaluate our model against typical attacks on existing BCS schemes.

Stolen Key Inversion Attack [12]: This attack bases on an assumption that the generated key has been compromised (which commonly occurs in practice).
 565 Then, the revealed key can be leveraged along with the helper data to learn a part (or all) of the biometric template. Then, all other BCS models of the

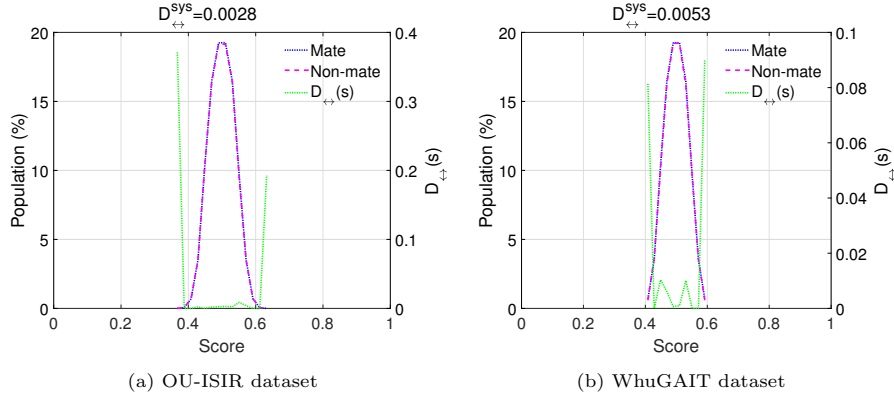


Figure 8: The unlinkability score measured on the reliable string ω .

target user will be permanently compromised. A BCS solution is vulnerable to this attack if it can not fulfill the irreversibility requirement. As analyzed in 4.4.4, in the IECO scheme, the attacker could not gain further advantage on
 570 reverting the original biometric data by observing the compromised key. Thus, our model is immune to the key inversion attack.

Record Multiplicity Attacks (RMA): These attacks exploit the correlation between multiple instances of helper data/key extracted from a same person (*e.g.*, FES [9], FVS [12], cancellable biometric [54]).

575 In FES [31], the XOR result of the biometric template and a codeword is stored as helper data. Then, given two helper data instances, the attacker can identify with high probability whether they are derived from a same user or not, by checking their XOR result [9]. This relied on a property of ECC which features that XOR-ing two valid codewords will result to a valid codeword.
 580 Thus, the XOR-ing of two helper data instances from a same user will be close to a valid codeword with high probability. It is clear that such attack is infeasible in our model, as we do not store the XOR result of the codeword and gait data.

In FVS, by matching two vaults (*i.e.*, helper data) derived from the same user, the biometric features could be identified [12]. This allows reconstructing
 585 the biometric data, and reveal the sealed key with high certainty. In our model, the biometric templates are covered by RP to provide unlinkability between

different enrollments. By matching two helper data instances, the attacker could not identify which locked points are from biometric features. Thus, the strategy of RMA used in FVS does not work on our model.

590 RMA also can be used to compromise the scheme that relies on RP to fulfill the irreversibility [54]. In such model, the irreversibility was addressed by a many-to-one linear system, in which, there are infinite solutions for a given pair of projected data and RP matrix. However, when the attacker can obtain multiple instances of transformed template and projection matrix, the original
595 template could be identified easily. In our model, the transformed template is not stored, but used for key generation. From the key, it is impractical to reconstruct the transformed template. Without the transformed template, the attacker could not revert to the original biometric data.

Statistical Attack: This attack targets the BCS models in which the extracted binary strings have low inter-class discrimination high intra-class variation
600 [11]. Due to the high intra-class variation, two-layer ECC is usually adopted to increase the error correcting capability [55]. In such model, the biometric binary string is equally divided into several chunks. The first ECC layer handles the error bit(s) in each chunk separately, then, the second layer corrects the
605 fault chunks by checking the consistency over all the chunks. Given the helper data, the attacker can try with a small biometric dataset. For each chunk, the histograms of output codewords is determined. The codeword corresponding to the highest bin of the histogram is then selected as the guessed codeword for the corresponding chunk [11]. In our model, due to the effectiveness of the
610 deep model, the extracted binary string ω features low intra-class variation and high inter-class separation (see 4). This allows the adoption of a long key and low-error-tolerant BCS scheme (*i.e.*, we use only one ECC layer). Thus, our model is secure against the statistical attack [50].

5.4.4. Comparison with Existing Works

615 To provide a meaningful comparison to existing gait cryptosystems [6, 7], we additionally experimented our model on CNU dataset [6], which has been

Table 2: A comparison on different factors between our model and existing gait cryptosystems, where R, I, and U mean Revocability, Irreversibility, and Unlinkability, respectively.

<i>Study</i>	<i>Data Length</i>	<i>Key size</i>	<i>Performance</i>	<i>R</i>	<i>I</i>	<i>U</i>
Hoang <i>et al.</i> 2015 [6]	16 cycles	139 bits	FAR: 0% FRR: 16.18%	-	-	-
Tran <i>et al.</i> 2017 [7]	26 cycles	148 bits	FAR: $6 \times 10^{-5}\%$ FRR: 9.2%	-	-	-
This study	5 cycles	139 bits	FAR: 0% FRR: 5.56%	Yes	Yes	Yes
		147 bits	FAR: 0% FRR: 7.64%			

used to evaluate their models. However, the gyroscope signal is not available on this dataset. Thus, we modified the network to accept the gait segment of 3 channels as the input (instead of 6 channels as in 4.2.1). Table 2 provides a comparison between our model and existing gait cryptosystems. It could be seen that, our model not only achieved higher performance, but also required smaller data segment for key reproduction. In addition, unlike existing schemes, we allowed key revocation, and fulfill irreversibility and unlinkability.

6. Conclusions

This study presented a novel gait cryptosystem to generate from sensor gait data a key for user authentication, meanwhile, secure the gait pattern. First, a deep network optimized by a new loss function was used to extract a representation template from the raw gait segment. Then, RP and feature-wise binarization were subsequently used to extract a revocable binary string. The string showed high stability when extracted from a same user, and great randomness between different users. Subsequently, an irreversible key was generated from the string, following the IECO scheme. The evaluation on OU-ISIR and whuGAIT datasets showed that our model was more secure and efficient comparing to existing gait BCSs. Moreover, our model was secure against existing biometric template protection attacks, and fulfilled the irreversibility and

unlinkability requirements.

Acknowledgments

The authors would like to thank Thang Hoang (Virginia Tech, USA) for helpful discussions and important references. This work was supported in part
640 by the Institute of Information & Communications Technology Planning & Evaluation (IITP) grant by the Korean Government, Ministry of Science and ICT (MSIT) under Grant 2020-0-00126, and in part by the Vietnam National University (VNU-HCM) under Grant NCM2019-18-01.

References

- 645 [1] S. Sprager, M. Juric, Inertial sensor-based gait recognition: a review, *Sensors* 15 (9) (2015) 22089–22127.
- [2] H. J. Ailisto, M. Lindholm, J. Mantyjarvi, E. Vildjiounaite, S.-M. Makela, Identifying people from gait pattern with accelerometers, in: *Biometric Technology for Human Identification II*, Vol. 5779, International Society
650 for Optics and Photonics, 2005, pp. 7–14.
- [3] C. Wan, L. Wang, V. V. Phoha, A survey on gait recognition, *ACM Computing Surveys (CSUR)* 51 (5) (2018) 1–35.
- [4] A. Sundararajan, A. I. Sarwat, A. Pons, A survey on modality characteristics, performance evaluation metrics, and security for traditional and
655 wearable biometric systems, *ACM Computing Surveys* 52 (2) (2019) 1–36.
- [5] C. Rathgeb, A. Uhl, A survey on biometric cryptosystems and cancelable biometrics, *EURASIP Journal on Information Security* 2011 (1) 1–25.
- [6] T. Hoang, D. Choi, T. Nguyen, Gait authentication on mobile phone using biometric cryptosystem and fuzzy commitment scheme, *International
660 Journal of Information Security* 14 (6) (2015) 549–560.

- [7] L. Tran, T. Hoang, T. Nguyen, D. Choi, Improving gait cryptosystem security using gray code quantization and linear discriminant analysis, in: Information Security Conference, Springer, 2017, pp. 214–229.
- [8] A. Juels, M. Wattenberg, A fuzzy commitment scheme, in: 6th ACM-CCS, 1999, pp. 28–36.
- 665
- [9] K. Simoons, P. Tuyls, B. Preneel, Privacy weaknesses in biometric sketches, in: 30th IEEE S&P, IEEE, 2009, pp. 188–203.
- [10] E. J. Kelkboom, J. Breebaart, T. A. Kevenaer, I. Buhan, R. N. Veldhuis, Preventing the decodability attack based cross-matching in a fuzzy commitment scheme, IEEE Transactions on Information Forensics and Security 6 (1) (2010) 107–121.
- 670
- [11] C. Rathgeb, A. Uhl, Statistical attack against iris-biometric fuzzy commitment schemes, in: CVPR 2011 WORKSHOPS, IEEE, 2011, pp. 23–30.
- [12] W. J. Scheirer, T. E. Boulton, Cracking fuzzy vaults and biometric encryption, in: 2007 Biometrics Symposium, IEEE, 2007, pp. 1–6.
- 675
- [13] ISO/IEC 24745:2011 Information technology – Security techniques – Biometric information protection, ISO, 2011.
- [14] R. Canetti, B. Fuller, O. Paneth, L. Reyzin, A. Smith, Reusable fuzzy extractors for low-entropy distributions, in: Annual International Conference on the Theory and Applications of Cryptographic Techniques, Springer, 2016, pp. 117–146.
- 680
- [15] W. B. Johnson, J. Lindenstrauss, Extensions of lipschitz mappings into a hilbert space, Contemporary mathematics 26 (189-206) (1984) 1.
- [16] T. T. Ngo, Y. Makihara, H. Nagahara, Y. Mukaigawa, Y. Yagi, The largest inertial sensor-based gait database and performance evaluation of gait-based personal authentication, Pattern Recognition 47 (1) (2014) 228–237.
- 685

- [17] Q. Zou, Y. Wang, Q. Wang, Y. Zhao, Q. Li, Deep learning-based gait recognition using smartphones in the wild, *IEEE Transactions on Information Forensics and Security* 15 (2020) 3197–3212.
- 690 [18] A. Bruesch, N. Nguyen, D. Schürmann, S. Sigg, L. Wolf, Security properties of gait for mobile device pairing, *IEEE Transactions on Mobile Computing* 19 (3) (2019) 697–710.
- [19] S. A. Niyogi, E. H. Adelson, et al., Analyzing and recognizing walking figures in xyt, in: *CVPR*, Vol. 94, 1994, pp. 469–474.
- 695 [20] L. Wang, T. Tan, H. Ning, W. Hu, Silhouette analysis-based gait recognition for human identification, *IEEE transactions on pattern analysis and machine intelligence* 25 (12) (2003) 1505–1518.
- [21] S. Sprager, M. B. Juric, An efficient hos-based gait authentication of accelerometer data, *IEEE transactions on information forensics and security* 700 10 (7) (2015) 1486–1498.
- [22] M. Gadaleta, M. Rossi, Idnet: Smartphone-based gait recognition with convolutional neural networks, *Pattern Recognition* 74 (2018) 25–37.
- [23] R. Subramanian, S. Sarkar, Evaluation of algorithms for orientation invariant inertial gait matching, *IEEE Transactions on Information Forensics and Security* 14 (2) (2019) 304–318.
- 705 [24] L. Tran, D. Choi, Data augmentation for inertial sensor-based gait deep neural network, *IEEE Access* 8 (2020) 12364–12378.
- [25] D. Gafurov, E. Snekenes, P. Bours, Gait authentication and identification using wearable accelerometer sensor, in: *2007 IEEE workshop on automatic identification advanced technologies*, IEEE, 2007, pp. 220–225.
- 710 [26] G. Trivino, A. Alvarez-Alvarez, G. Bailador, Application of the computational theory of perceptions to human gait pattern recognition, *Pattern Recognition* 43 (7) (2010) 2572–2581.

- [27] B. Sun, Y. Wang, J. Banda, Gait characteristic analysis and identification based on the iphone's accelerometer and gyrometer, *Sensors* 14 (9) (2014) 17037–17054.
- [28] G. Giorgi, F. Martinelli, A. Saracino, M. Sheikhalishahi, Try walking in my shoes, if you can: Accurate gait recognition through deep learning, in: *International Conference on Computer Safety, Reliability, and Security*, Springer, 2017, pp. 384–395.
- [29] O. Dehzangi, M. Taherisadr, R. ChangalVala, Imu-based gait recognition using convolutional neural networks and multi-sensor fusion, *Sensors* 17 (12) (2017) 2735.
- [30] F. J. MacWilliams, N. J. A. Sloane, *The theory of error correcting codes*, Vol. 16, Elsevier, 1977.
- [31] Y. Dodis, R. Ostrovsky, L. Reyzin, A. Smith, Fuzzy extractors: How to generate strong keys from biometrics and other noisy data, *SIAM journal on computing* 38 (1) (2008) 97–139.
- [32] A. Juels, M. Sudan, A fuzzy vault scheme, *Designs, Codes and Cryptography* 38 (2) (2006) 237–257.
- [33] M. Blanton, M. Aliasgari, Analysis of reusability of secure sketches and fuzzy extractors, *IEEE transactions on information forensics and security* 8 (9) (2013) 1433–1445.
- [34] X. Boyen, Reusable cryptographic fuzzy extractors, in: *11th ACM conference on Computer and Communications Security*, 2004, pp. 82–91.
- [35] D. Apon, C. Cho, K. Eldefrawy, J. Katz, Efficient, reusable fuzzy extractors from lwe, in: *International Conference on Cyber Security Cryptography and Machine Learning*, Springer, 2017, pp. 1–18.
- [36] R. Canetti, Y. T. Kalai, M. Varia, D. Wichs, On symmetric encryption and point obfuscation, in: *Theory of Cryptography Conference*, Springer, 2010, pp. 52–71.

- [37] J. H. Cheon, J. Jeong, D. Kim, J. Lee, A reusable fuzzy extractor with practical storage size: Modifying canetti et al.'s construction, in: Australasian Conference on Information Security and Privacy, Springer, 2018, pp. 28–44.
- 745 [38] F. Zhu, P. Shen, C. Chen, A performance-optimization method for reusable fuzzy extractor based on block error distribution of iris trait, in: International Conference on Security and Privacy in Communication Systems, Springer, 2019, pp. 259–272.
- [39] L. Chen, T. M. Laing, K. M. Martin, Efficient, xor-based, ideal (t, n) -
750 threshold schemes, in: International Conference on Cryptology and Network Security, Springer, 2016, pp. 467–483.
- [40] G. Panchal, D. Samanta, A novel approach to fingerprint biometric-based cryptographic key generation and its applications to storage security, Computers & Electrical Engineering 69 (2018) 461–478.
- 755 [41] A. Anees, Y.-P. P. Chen, Discriminative binary feature learning and quantization in biometric key generation, Pattern Recognition 77 (2018) 289–305.
- [42] V. Talreja, M. C. Valenti, N. M. Nasrabadi, Deep hashing for secure multimodal biometrics, IEEE Transactions on Information Forensics and Security 16 (2020) 1306–1321.
- 760 [43] B. Lynn, M. Prabhakaran, A. Sahai, Positive results and techniques for obfuscation, in: International conference on the theory and applications of cryptographic techniques, Springer, 2004, pp. 20–39.
- [44] L. Tran, T. Hoang, T. Nguyen, H. Kim, D. Choi, Multi-model long short-term memory network for gait recognition using window-based data segment,
765 IEEE Access 9 (2021) 23826–23839.
- [45] I. J. Schoenberg, Cardinal spline interpolation, SIAM, 1973.
- [46] R. Delgado-Escañó, F. M. Castro, J. R. Cózar, M. J. Marín-Jiménez, N. Guil, An end-to-end multi-task and fusion cnn for inertial-based gait recognition, IEEE Access 7 (2018) 1897–1908.

- 770 [47] Y. Chen, Z. Lai, Y. Ding, K. Lin, W. K. Wong, Deep supervised hashing with anchor graph, in: ICCV, 2019, pp. 9796–9804.
- [48] L. Ma, X. Li, Y. Shi, L. Huang, Z. Huang, J. Wu, Learning discrete class-specific prototypes for deep semantic hashing, *Neurocomputing* 443 (2021) 85–95.
- 775 [49] F. Schroff, D. Kalenichenko, J. Philbin, Facenet: A unified embedding for face recognition and clustering, in: CVPR, 2015, pp. 815–823.
- [50] A. Stoianov, T. Kevenaar, M. Van der Veen, Security issues of biometric encryption, in: 2009 IEEE Toronto International Conference Science and Technology for Humanity (TIC-STH), IEEE, 2009, pp. 34–39.
- 780 [51] L. Van der Maaten, G. Hinton, Visualizing data using t-sne., *Journal of machine learning research* 9 (11).
- [52] M. Osadchy, O. Dunkelman, It is all in the system’s parameters: Privacy and security issues in transforming biometric raw data into binary strings, *IEEE Transactions on Dependable and Secure Computing* 16 (5) (2018) 796–804.
- 785 [53] M. Gomez-Barrero, J. Galbally, C. Rathgeb, C. Busch, General framework to evaluate unlinkability in biometric template protection systems, *IEEE Transactions on Information Forensics and Security* 13 (6) (2017) 1406–1420.
- 790 [54] C. Li, J. Hu, Attacks via record multiplicity on cancelable biometrics templates, *Concurrency and Computation: Practice and Experience* 26 (8) (2014) 1593–1605.
- [55] F. Hao, R. Anderson, J. Daugman, Combining crypto with biometrics effectively, *IEEE transactions on computers* 55 (9) (2006) 1081–1088.